P-ISSN 2586-9000
E-ISSN 2586-9027
Homepage : https://tci-thaijo.org/index.php/SciTechAsia
Science & Technology Asia
Vol.28 No.4 October - December 2023
Page: [11-19]
Original research article

Heat Transfer Analysis in an Unsteady MHD Flow over a Stretchable Permeable Surface under Ohmic Heating and Viscous Dissipation

Bhaskarjyoti Deka*, Rita Choudhury

Department of Mathematics, Gauhati University, Assam 781014, India

Received 22 July 2023; Received in revised form 25 September 2023
Accepted 10 October 2023; Available online 27 December 2023

ABSTRACT

This work aims to study the two-dimensional unsteady problem of an incompressible, electrically conductive, viscous fluid over a stretchable and permeable surface. The effects of unsteadiness in the flow and temperature fields in the presence of Joule heating, viscous dissipation, and heat source have been analyzed. Similar transformations transform the boundary layer equations of momentum and heat transfer into nonlinear ordinary differential equations. A set of ordinary differential equations is solved using a numerical technique. The effects of various relevant flow parameters on the flow and heat transfer properties are displayed in several graphs and tables. Comparisons with previous studies have been made, and conformity is noticed. Applications of such models have been noted in various engineering and industrial schemes.

Keywords: Boundary layer; MHD; Permeable surface; Stretching surface; Unsteady flow

1. Introduction

In recent decades, numerous analysts have broadly centered on hydromagnetic flux development in electrically conducting fluid over a stretching surface. This is due to their far-reaching application in mechanical fabricating, cutting-edge metallurgical and metal-working forms like hot lamination, glass forming technique, papermaking, wire and plastic sheet drawing, etc. Within the field of mechanical designing, magnetohydrodynamics is often used for plasma control, fluid alloy cooling of atomic reactors, and metal pitching. By ideals of broadened scholastic and exploratory conspicuousness, characteristics of the previously mentioned streams have been assessed by numerous researchers, viz. Pavlov [1], Andersson [2], Liu [3] etc.

***Corresponding author:** bhaskarjyoti9931@gmail.com

Fluid flow over-stretching surfaces takes various design forms with viable applications in areas such as glass blowing, cooper spirals, wire drawing, etc. Sakiadis [4] progressed a stream field with a continuous flat surface in a stationary fluid moving steadily. A viscous stream in a convective boundary layer past a direct stretchable layer has been considered by Crane [5] and displayed a closed exponential arrangement to the demonstrated condition. Afzal and Varshney [6] amplified the Crane [5] issue as a common stretching control law, and Ali [7] considered the accustomed case where a sheet stretches at a specific shape of stretching rate.

The Ohmic heating and viscous dissipation behaviors in different streams are critical in upgrading heat exchange properties. Dissipated thermal energy performs an essential role in increasing the viscidity of fluid. Dissipation is not easily ignored, especially for polymer manufacturing, which occurs at high temperatures. Nyamai [8] discussed the Hartmann number impact in a flat plate moving with steady speed, viscous dissipation, and Joule heating. Mishra and Mohanty [9] analyzed the impression of Ohmic heating and chemical reaction over a stretching surface. They used the Darcy-Forchheimer drag model to re-enact second-order permeable drag impacts. The flow of an unsteady MHD viscous fluid across a horizontal stretching sheet is investigated by Quasim et al. [10] for the effect of Ohmic heating. They employed the Gear-Generalized Differential Quadrature method to solve commanding equations. Kumbhakar et al. [11] inspected the viewpoints of the unsteady stream of crossover nanofluid over a convectively warmed stretching cylinder under the impact of the diagonal Lorentz drive and viscous dissipation.

The issue of steady and unsteady laminar flow on permeable surfaces has been an essential theme in fluid flow, as it is considered necessary and comprehensive from both hypothetical and practical frames of reference. In addition, there are various applications in engineering and mechanical forms, viz., oil companies, polymer film ejection from a colour, groundwater stream, etc. The traits of preceding flow over porous surfaces have been assessed by many analysts, viz. [12-19] in a state of constraining cases. Furthermore, the sequels of heat transmission on unsteady flow through a stretching surface have been demonstrated by several researchers, viz. [20-27].

Based on the above, we explore an unsteady MHD viscous fluid stream over a stretching surface implanted with a permeable medium. Furthermore, the energy equation considers outcomes of dissipated thermal energy, specifically Ohmic heating and viscous dissipation. In addition, a uniform heat source is considered to enrich the problem. Using an appropriate homothetic transformation, the problem is transformed, and the transmuted equations are decomposed into sets. Nonlinear coupled ordinary differential equations are solved numerically using the bvp4c solver of MATLAB. The response of the distinctive parameters is considered graphically, and the calculation comes about of the physical coefficients being distinguished and displayed in tabular shape. The solutions above are accepted by comparison with what has already been obtained and give affirmation for advanced studies. Exploring unsteady flow on extended permeable surfaces provides insights into fluid dynamics, mathematical modeling, flow control, and industrial applications in various fields, including film production, metal processing, fiber spinning, paper production, and food processing.

2. Formulation of the Problem

The main objective of this segment is to describe the equations governing laminar boundary layer fluid flow in two-dimensional electrically conducting

incompressible viscous flow and heat transmission through an unsteady stretching permeable surface.

We consider physical properties such as stretching velocity $U_w(x,t)$ and surface temperature $T_w(x,t)$; these are supposed to be universal. The external fluid is presumed negligible due to charge polarization and the Hall effect. The origin is adjusted in a fluid with ambient temperature T_∞ at $t=0$ and the surface is impetuously prolonged along the *x*-axis by velocity $U_\infty(x,t)$. In the rectangular coordinate system, the positive *x*-axis extends along the surface, and the *y*-axis is scaled perpendicular to the surface, wherein a transversal magnetic field of constant strength B_0 is implemented with the positive *y*-axis normal to the surface such that the induced field is negligible, assuming a small magnetic Reynolds number.

The commanding equations that characterize the physical situation are shown as:

$$\frac{\partial u}{\partial x}+\frac{\partial v}{\partial y}=0, \tag{2.1}$$

$$\frac{\partial u}{\partial t}+u\frac{\partial u}{\partial x}+v\frac{\partial u}{\partial y}=v\frac{\partial^2 u}{\partial y^2}-\frac{\sigma B_0^2 u}{\rho}-\frac{vu}{\kappa_0}+g\beta(T-T_\infty), \tag{2.2}$$

$$\frac{\partial T}{\partial t}+u\frac{\partial T}{\partial x}+v\frac{\partial T}{\partial y}=\alpha\frac{\partial^2 T}{\partial y^2}+\frac{\sigma B_0^2 u^2}{\rho C_p}+\frac{\mu}{\rho C_p}\left(\frac{\partial u}{\partial y}\right)^2+\frac{Q}{\rho C_p}(T-T_\infty), \tag{2.3}$$

where $u \& v$ are the velocity components along tangential & normal directions, t is dimensional time, v is kinematic viscosity, σ is electrical conductivity, ρ is mass density, κ_0 is permeability of porous medium, g is gravitational acceleration, T is fluid temperature, α is thermal diffusivity, C_p is specific heat capacity at constant pressure, μ is coefficient of viscosity, Q is coefficient of heat generation.

The following limiting conditions apply to Eqs. (2.1)-(2.3);

$$y=0: u=U_w, v=0, T=T_w,$$
$$y\to\infty: u\to 0, T\to T_\infty, \tag{2.4}$$

where stretching velocity $U_w(x,t)$ and surface temperature $T_w(x,t)$ can be defined as:

$$U_w(x,t)=\frac{ax}{1-ct},$$
$$T_w(x,t)=T_\infty+\frac{bx}{1-ct}. \tag{2.5}$$

Here $a,b \& c$ are constants including $a>0, b\geq 0 \& c\geq 0$ with $ct<1$; two positive constants $a \& b$ have dimension t^{-1} to obtain the dimension of the velocity. At $t=0$ (first motion), Eqs. (2.1)-(2.3) represent steady flow along the stretching surface. This special form of $U_w(x,t)$ and $T_w(x,t)$ has been picked to allow us to develop new similarity transformations that transform the dominant partial differential equations into a set of ordinary ones. This facilitates the study of the influence of control parameters. To obtain a similar solution to the equation, further assume that the unsteady magnetic field has the form $B=\frac{B_0}{\sqrt{1-ct}}$; the term B_0 is a constant.

The transport equation mentioned earlier in Eq. (2.1) is similarly contented by initiating a stream function $\Psi(x,y)$ so as $(u,v)=\left(\frac{\partial\Psi}{\partial y},-\frac{\partial\Psi}{\partial x}\right)$.

The underlying Eqs. (2.1)-(2.3) are reduced by developing following transformations:

$$\eta=\sqrt{\frac{U_w}{vx}}y, \Psi=\sqrt{vxU_w}f(\eta), \theta(\eta)=\frac{T-T_\infty}{T_w-T_\infty}, \tag{2.6}$$

where η is the transformed coordinate, $\theta(\eta)$ is dimensionless temperature, and $f(\eta)$ is dimensionless stream function.

The system of Eqs. (2.2)-(2.3) are transformed to dimensionless mode as:

$$f''' + ff'' - f'^2 - Mf' - A\left(f' + \frac{1}{2}\eta f''\right) - S_p f' + Gr\theta = 0, \tag{2.7}$$

$$\frac{\theta''}{Pr} + f\theta' - f'\theta + EcMf'^2 + Ecf''^2 + S\theta - A\left(\theta + \frac{1}{2}\eta\theta'\right) = 0, \tag{2.8}$$

The transmuted boundary conditions are:

$$\eta = 0 : f(\eta) = 0, f'(\eta) = 1, \theta(\eta) = 1,$$
$$\eta \to \infty : f'(\eta) \to 0, \theta(\eta) \to 0. \tag{2.9}$$

Furthermore, the dimensionless quantities appearing in Eqs. (2.7)-(2.8) above are mathematically defined as follows:

$$M = \frac{\sigma B^2}{\rho a}, S_p = \frac{v}{\rho a}, Pr = \frac{v}{a}, Gr = \frac{g\beta x(T_w - T_\infty)}{U_w^2},$$
$$A = \frac{c}{a}, S = \frac{Qx}{\rho C_p U_w}, \kappa_0 = \rho(1 - ct), Ec = \frac{U_w^2}{C_p(T_w - T_\infty)}. \tag{2.10}$$

The properties of flow circumstances, i.e., physical coefficients such as local skin friction coefficient (C_{fx}) and local Nusselt number (Nu_x) are defined respectively as:

$$C_{fx} = \frac{\tau_w}{\rho U_w^2/2}, \text{ then } C_{fx} = 2Re_x^{-1/2} f''(0),$$

$$Nu_x = \frac{1}{\kappa}\frac{xq_w}{(T_w - T_\infty)}, \text{ then } Nu_x = -Re_x^{-1/2}\theta'(0),$$

where Reynolds number $Re_x = \frac{U_w x}{v}$,

Skin friction coefficient $\tau_w = \mu\left(\frac{\partial u}{\partial y}\right)_{y=0}$,

Heat transfer from the surface

$$q_w = -\kappa\left(\frac{\partial T}{\partial y}\right)_{y=0}.$$

3. Solution Scheme

The commanding partial differential Eqs. (2.2)-(2.3), together with their analogous limiting conditions Eq. (2.4), require several subjects to various conditions on account of unsteadiness and its nonlinear dynamic behaviour. Simplifications and appropriate similarity transformations are performed before being mathematically solved using a numerical tool. To this end, the subsequent set of ordinary differential Eqs. (2.7)-(2.8), along with the transformed limiting conditions Eq. (2.9), are numerically solved using a bvp4c solver built into MATLAB. It provides a numerical solution for the two-point boundary value problem. The plot shows the numerical solution for divergent parameters that influence the problem.

4. Results and Discussion

A wide range of parameters may need to be explored, and the calculations prove to be particularly complex when the values of relevant parameters are significant, as they cannot converge numerically. As a result, this section presents results for a finite range of physical parameters picked to illustrate the important trends. Continuing from the preceding part, we calculated the distinctive parameters that embody the flow aspects, as shown in Figs. 1-10 and Tables 1-2. To fully understand the phenomena involved in heat and mass transfer problems, it is essential to understand the decision variables that control these processes and their physical explanations. As input for obtaining the entire production outcome, the values of the parameters are $M = 0.5, S_p = 0.4, A = 1,$ $Gr = 5, Pr = 7, Ec = 0.05, S = 3, \eta = 2$ except differently specified.

Figs. 1-6 show velocity distribution profiles that explain the behaviour of some distinctive parameters.

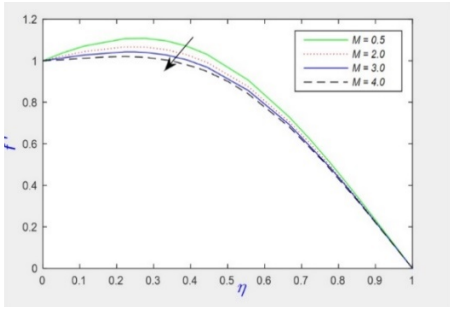

Fig. 1. Velocity distribution for different values of M with $Pr = 7, Gr = 5, \eta = 2, S_p = 0.4, A = 1, Ec = 0.05, S = 3.$

Fig. 1 is a pictorial depiction of the velocity profile for divergent values of magnetic parameter (M). It is conceivable that the velocity profile decreases as the value of the magnetic parameter increases. The decrease in fluid momentum is caused by the dual influence of magnetic and electric forces within the conducting fluid, and the enforced magnetic field produces an opposing force called the Lorentz force, which is opposite to the flow direction; as a result, the velocity of the fluid decreases.

Fig. 2 exhibits the behaviour of unsteady parameter (A) on fluid mobility. It can be seen that the velocity decreases as the unsteady parameter increases. A decrease abets this result in the thickness of the momentum boundary layer within the profile, and this suggests that the unsteady parameter cuts down the flow velocity because of the stretching sheet.

The influence of Eckert number (Ec) and porosity parameter (S_p) on fluid velocity are elucidated in Figs. 3-4, respectively. Numerical findings in Fig. 3 display that the momentum transport increases with increasing Eckert number, while in Fig. 4, it can be seen that velocity decreases as the porosity parameter increases. The porosity parameter hinders fluid movement through the surface, thus providing resistance to the flow. As the value of the porosity parameter rises, the momentum boundary layer thickness upsurges, so the velocity profile reduces, and it is because of the matter that the effect of the flow-blocking permeable media is also increased, increasing flow deceleration.

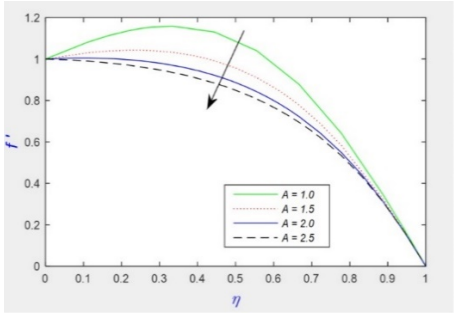

Fig. 2. Velocity distribution for different values of A with $Pr = 7, Gr = 5, \eta = 2, S_p = 0.4, S = 3, Ec = 0.05.$

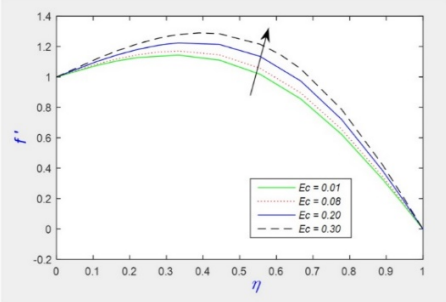

Fig. 3. Velocity distribution for different values of Ec with $Pr = 7, Gr = 5, \eta = 2, S_p = 0.4, M = 0.5, A = 1, S = 3.$

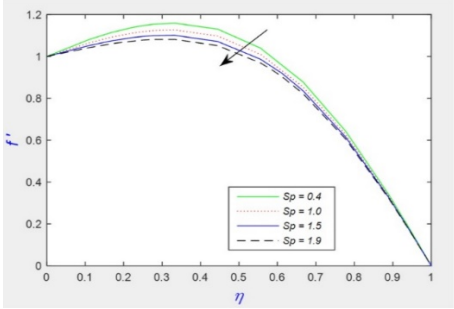

Fig. 4. Velocity distribution for different values of S_p with $Pr = 7, Gr = 5, \eta = 2, M = 0.5, A = 1, Ec = 0.05, S = 3.$

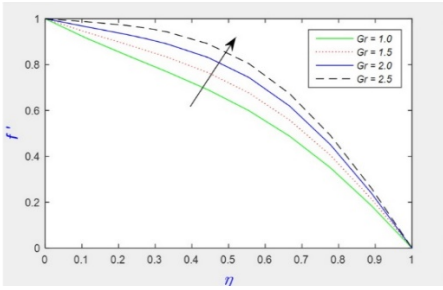

Fig. 5. Velocity distribution for different values of Gr with $Pr = 7, M = 0.5, \eta = 2, S_p = 0.4, A = 1,$ $Ec = 0.05, S = 3.$

The behaviour of the thermal Grashof number (Gr) and heat source parameter (S) are presented in Figs. 5-6, respectively. Interestingly, both parameters increase the momentum of the fluid. Fig. 6 displays that with the increasing value of the heat source parameter, the solidity of the thermal boundary layer increases, and as a result, the fluid velocity is enhanced.

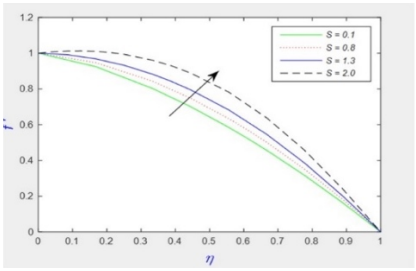

Fig. 6. Velocity distribution for different values of S with $Pr = 7, M = 0.5, \eta = 2, S_p = 0.4, A = 1,$ $Ec = 0.05, Gr = 5.$

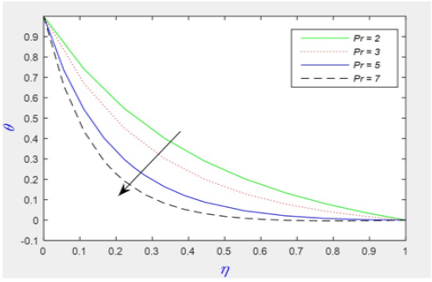

Fig. 7. Temperature profile for different values of Pr with $Gr = 5, M = 0.5, \eta = 2, S_p = 0.4, A = 1,$ $Ec = 0.05, S = 3.$

The characteristic of different parameters related to heat has been shown in Figs. 7-10.

In Fig. 7, we can see the impression of the Prandtl number (Pr) on the temperature field. An escalation in the Prandtl number increases fluid viscosity, which increases the fluid density and lowers the temperature profile.

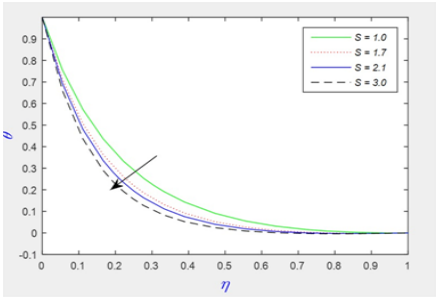

Fig. 8. Temperature profile for different values of S with $Pr = 7, M = 0.5, \eta = 2, S_p = 0.4, A = 1,$ $Ec = 0.05, Gr = 5.$

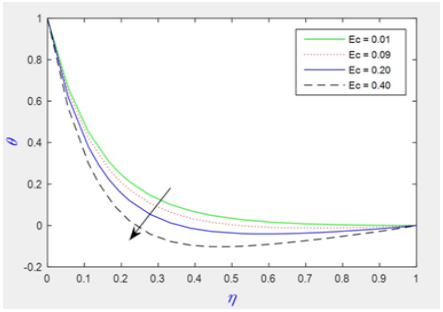

Fig. 9. Temperature profile for different values of Ec with $Pr = 7, Gr = 5, \eta = 2, S_p = 0.4, M = 0.5,$ $A = 1, S = 3.$

The fall of the temperature distribution with the increment of the heat source parameter (S) is shown in Fig. 8. The rise in the field temperature is expected because of the increase in the value of the heat source parameter. Still, a conflicting result has been found due to the influence of outward temperature.

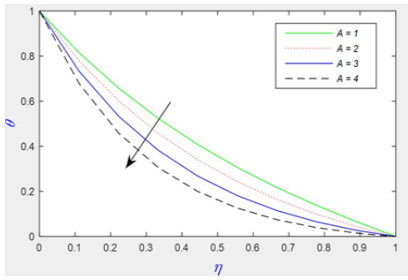

Fig. 10. Temperature profile for different values of A with $Pr = 7, Gr = 5, \eta = 2, S_p = 0.4, S = 3, Ec = 0.05$.

Figs. 9-10 exhibit the effects of Eckert number and unsteady parameter on temperature profile. Fig. 9 shows that the temperature drops as the Eckert number (Ec) increases. Moreover, Fig. 10 shows the consequence of the unsteady parameter (A) on heat dissipation. It can be seen that the temperature sketch drops substantially as the unsteady parameter increases. This is because the increased instability boosts the heat loss on account of surface elongation and consequently reduces the temperature, and this means that the cooling rates are much more rapidly related to the steady-flow cooling rate because at large values of unsteady parameter, heat transmission from the surface to the fluid decreases.

A significant influence of flow parameters on skin friction coefficient is observed in Table 1.

Table 1. Coefficient of skin friction (τ) for variations of different parameters.

Pr	M	Gr	S_p	S	A	Ec	τ
7	0.5	5	0.4	3	1	0.05	0.7505
	2.0						0.4402
	3.0						0.2458
	4.0						0.0601
7	0.5	2.5	0.4	3	1.0	0.05	-0.1227
					1.5		-0.4532
					2.0		-0.5708
					2.5		-0.6308
7	0.5	5	0.4	2	1	0.05	0.2253
			1.0				0.0610
			1.5				-0.0705
			1.9				-0.1724
7	0.5	1.0	0.4	3	1	0.05	-1.1569
		1.5					-0.9173
		2.0					-0.6948
		2.5					-0.4850

It is seen that an increase in the magnetic parameter reduces the skin friction coefficient. This suggests that the application of transverse magnetism cancels the frictional drag significantly. Therefore, the viscous resistance due to the appliance of the magnetic field is suppressed.

Also, the coefficient of skin friction decreases as the unsteady and porosity parameters increase and increase as the thermal Grashof number increases. In Table 1, we see a negative value for the skin friction coefficient, which means that the solid surface applies resistance to the fluid. This is because the stretching surface exclusively drives the growth of the momentum boundary layer. Moreover, we find that the momentum decreases with increasing distance from the surface, asymptotically to the limiting conditions at infinity.

Table 2 shows that the Nusselt number changes as the flow rate parameter is varied.

Table 2. Nusselt Number (Nu) for variations of different parameters.

Pr	M	Gr	S_p	S	A	Ec	Nu
7	0.5	5	0.4	3	1	0.05	-7.5927
					2		-13.9464
					3		-20.8108
					4		-27.7804
7	0.5	5	0.4	1.0	1	0.05	-5.1429
				.7			-6.2511
				2.1			-6.7244
				3.0			-7.5927
2	0.5	5	0.4	3	1	0.09	-2.7502
3							-3.7169
5							-5.7350
7							-7.8089
7	0.5	5	0.4	3	1	0.01	-7.3802
						0.09	-7.8089
						0.20	-8.4232
						0.40	-9.6202

The Nusselt number appears in a descending trend with parameters like an unsteady parameter, heat source parameter, Prandtl number, and Eckert number. From a physical point of view, the negative value of the Nusselt number in Table 2 refers to the fact that heat passes off the surface for all considered distinctive parameters.

It can be observed that the trends in the graphs and tables in this study are very

comparable to those of Jhankal et al. [13] and Ishak [20].

5. Conclusion

A numerical solution has been attained to examine the consequence of varying properties of divergent parameters on the time-dependent incompressible MHD flow of fluids across stretchable surfaces enclosed in a homogenous porous media, the obtained ordinary differential equations describing the problem have been solved numerically. Visual representations through figures generated from numerical calculations help to identify the impacts of relevant flow parameters on flow and heat transfer. The numerical values of the coefficient of skin friction and rate of heat transmission are acquired for disparate values of parameters and represented via tables.

It is observed that both unsteady and porosity parameters have an opposite relationship with the velocity profile and coefficient of local skin friction. The heat source parameter and Eckert number have an absolute connection with the fluid mobility, i. e. , the velocity field increases when the effects of these parameters are considered.

We have perceived that heat distribution is less dependent on the values of the unsteady parameter and Eckert number as the temperature profile was found to be decreased with the variation of these parameters. Moreover, the heat source and unsteady parameters effectively impede the heat transfer rate from the surface.

The results obtained here are comparable with the earlier noted cases.

References

[1] Pavlov KB. Magnetohydrodynamic flow of an incompressible viscous fluid caused by deformation of a plane surface. Magnitnaya Gidrodinamika 1974; 10:146-8.

[2] Andersson HI. An exact solution of the Navier-Stokes equation for magnetohydrodynamic flow. Acta Mechanica 1995; 113:241-4.

[3] Liu IC. A note on heat and mass transfer for a hydromagnetic flow over a stretching sheet. Heat Mass Transfer 2005; 32:1075-84.

[4] Sakiadis BC. Boundary-layer behavior on continuous solid surfaces: II The boundary layer on a continuous flat surface. AIchE Journal 1961; 7(2):221-5.

[5] Crane LJ. Flow past a stretching sheet. Zeitschrift fur Angewandte Mathematik und Physik 1970; 21:645-7.

[6] Afzal N, Varshney IS. The cooling of a low resistance stretching sheet moving through a fluid. Heat Mass Transfer 1980; 14:289-93.

[7] Ali ME. On thermal boundary layer on a power- law stretched surface with suction or injection. Int J Heat Fluid Flow 1995; 16:280-90.

[8] Nyamai BM. Modelling the effect of Hartmann number on transient period, viscous dissipation and Joule heating in a transient MHD flow over a flat plate moving at a constant velocity. Journal of Advances in Mathematics and Computer Science 2019;33(3):1-10.

[9] Mishra S, Mohanty B. Heat and mass transfer flow over a stretching surface with Ohmic heating and chemical reaction. Heat Transfer 2020;49: 3837-53.

[10] Qasim M, Afridi MI, Wakif A, Thoi TN, Hussanan A. Second law analysis of unsteady MHD viscous flow over a horizontal stretching sheet heated non-uniformly in the presence of Ohmic heating: utilization of Gear- Generalised Differential Quadrature Method. Entropy 2019; 21:240 doi:10.3390/e21030240.

[11] Kumbhakar B, Nandi S, Chamkha AJ. Unsteady hybrid nanofluid flow over a convectively heated cylinder with inclined magnetic field and viscous dissipation: A

multiple regression analysis. Chinese Journal of Physics 2022; 79:38-56.

[12] Choudhury MK, Choudhury S, Sharma R. Unsteady MHD flow and heat transfer over a stretching permeable surface with suction or injection. International Conference on Computational Heat and Mass Transfer, Procedia Engineering 2015: 127:703-10.

[13] Jhankal AK, Jat RN, Kumar D. Unsteady MHD flow and heat transfer over a porous stretching plate. International Journal of Computational and Applied Mathematics 2017;12(2):325-33.

[14] Oyelakin IS, Mondal S, Sibanda P. Unsteady MHD three-dimensional Casson nanofluid flow over a porous linear stretching sheet with slip condition. Frontiers in Heat and Mass Transfer 2017; 8:37.

[15] Ishak A, Nazar R, Pop I. Heat transfer over an unsteady stretching permeable surface with prescribed wall temperature. Nonlinear Anal. RWA 2009; 10:2909-13.

[16] Cortell R. Combined effect of viscous dissipation and thermal radiation on fluid flows over a non- linearly stretched permeable wall. Meccanica 2012; 47:769-81.

[17] Khader MM. Laguerre collocation method for the flow and heat transfer due to a permeable stretching surface embedded in a porous medium with a second order slip and viscous dissipation. Appl. Math. Compute. 2014; 243:503-13.

[18] Das M, Mahanta G, Shaw S. Heat and mass transfer effect on an unsteady MHD radiative chemically reactive Casson fluid over a stretching sheet in porous medium. Heat Transfer 2020; 49:4350-69.

[19] Krishna MV, Reddy MG, Chamkha AJ. Heat and mass transfer on unsteady MHD flow through an infinite oscillating vertical porous surface. Journal of Porous Media 2021; 24(1): 81-100.

[20] Ishak A. Unsteady MHD flow and heat transfer over a stretching plate. Journal of Applied Sciences 2010;10(18):2127-31.

[21] Gupta PS, Gupta AS. Heat and mass transfer on a stretching sheet with suction or blowing. Can J Chem Eng 1977; 55:744-6.

[22] Elbashbeshy EMA, Bazid MAA. Heat transfer over an unsteady stretching surface. Heat Mass Transfer 2004; 41:1-4.

[23] Tsai R, Huang KH, Huang JS. Flow and heat transfer over an unsteady stretching surface with non- uniform heat source. Heat Mass transfer 2008; 35:1340-3.

[24] Takhar HS, Nath G. Unsteady flow over a stretching surface with a magnetic field in a rotating fluid. ZAMP 1998; 49: 989-1001.

[25] Ahmed MM, Ghoneim NI, Reddy MG, El-Khatib M. Magnetohydrodynamic fluid flow due to an unsteady stretching sheet with thermal radiation, porous medium and variable heat flux. Advances in Astronomy 2021: https://doi.org/10.1155/2021/6686883

[26] Noor NFM, Abdulaziz, Hashim I. MHD flow and heat transfer in a thin liquid film on an unsteady stretching sheet by the homotopy analysis method. Int J for Numerical methods in Fluids 2010; 63:357-73.

[27] Megahed AM, Reddy MG, Abbas W. Modeling of MHD fluid flow over an unsteady stretching sheet with thermal radiation, variable fluid properties and heat flux. Mathematics and Computers in Simulation 2021; 185: 583-93.